Proceedings of the 21st ICSMGE, Vienna, Austria, 14 – 19 June 2026. Pistrol, Adam & Schweiger (eds.)
Published by: ÖGG, Austrian Society for Geomechanics, Salzburg, Austria, ISBN 978-3-9503898-4-5
https://doi.org/10.53243/ICSMGE2026-1048

Assessing suffusion of sand-clay mixtures through laboratory experiments

Junhyeok Kwak, Chaemin Kim, Jongmuk Won
Department of Civil, Environmental and Architectural Engineering, Korea University, 145, Anam-ro, Seongbuk-gu, Seoul 02841, South Korea, jmwon@korea.ac.kr

ABSTRACT: Suffusion is the loss of relatively small particles caused by water flow, which can potentially downgrade the integrity of geotechnical infrastructure. Because most of the previous studies focused on investigating the suffusion of gap-graded coarse-grained soils, this study introduces the assessment of suffusion of sand-clay mixtures under two-dimensional flow through laboratory experiments. The impact of clay type, size ratio, and ionic concentration on the suffusion of sand-clay mixtures under gradual increase in flow rate was investigated through the total mass of filtrated clay. In addition, the impact of biopolymer treatment was also discussed to assess the optimal biopolymer type and biopolymer concentration in mitigating the suffusion of clay particles. It was found that the swelling clay showed lower susceptibility to suffusion than non-swelling clay, in which all clay types showed a critical hydraulic gradient of less than 1. In addition, the mitigation of suffusion by biopolymer treatment was in the order of samples treated by guar gum, chitosan, agar gum, xanthan gum, and gellan gum.

KEYWORDS: suffusion, biopolymer treatment, two-dimensional flow, sand-clay mixture, clay type

1 INTRODUCTION

The suffusion is primarily caused by seepage forces applied to small particles, while the large particles remain stationary without losing contact between particles (Fannin & Slangen 2014; Hunter & Bowman 2018; Ke & Takahashi 2014). The occurrence of suffusion progressively enlarges the pore sizes of the soil matrix, which leads to an increase in hydraulic conductivity and a reduction in the stiffness of soils (Chen et al., 2021; Xiong et al., 2021; Xu et al., 2021). Therefore, the long-term suffusion can trigger geotechnical failures, including land subsidence, and the failure of earth dams (Adamo et al. 2020; Nam 2019; Wan & Fell 2008).

Suffusion has been conducted through investigations of various approaches, including laboratory experiments (Won et al., 2023), field investigations (Parekh, 2016), and numerical modelling (Tao & Tao, 2017). However, most laboratory studies have been carried out for suffusion under one-dimensional flow, which may not explain suffusion under two- or three-dimensional flows. The detached small particles are subjected to reattachment and gravitational forces during their transport through the soil matrix. Therefore, the objective of this study is to investigate the suffusion behavior of sand-clay mixtures using a two-dimensional flow cell. Experiments were conducted under a constant flow rate to evaluate the effects of ionic concentration (IC), particle size ratio (SR), and clay type on suffusion behavior under two-dimensional flow. Subsequently, the critical hydraulic gradient (i_{cr}) was examined under a gradually increasing flow rate condition. In addition, an impact of biopolymer treatment on the mitigation of suffusion using five types of biopolymers (Xanthan gum, Agar gum, Gellan gum, Chitosan, and Guar gum) was also investigated.

2 MATERIALS AND METHOD

2.1 *Materials*

In this study, three sands (K3, K4, and K5) and clays (kaolinite, illite, and bentonite) were selected to investigate the effect of size ratio (SR) between sand and clay, clay mineralogy (1:1 or 2:1 clay), and swelling potential on suffusion of sand-clay mixtures. The particle size distributions of sand and clay were determined via sieve analysis (ASTM D422) and the laser diffraction method (Horiba LA-960), respectively. Specific gravity, maximum void ratio, and minimum void ratio were determined using a pycnometer (ASTM D854), funnel deposition method (ASTM D4253), and vibrating table method (ASTM D4254), respectively. The roundness of K3, K4, and K5 sand was higher than 0.7 (measured by image analysis) and the particle size distribution of the three sands indicates that the sand used in this study is uniform, rounded sand. All physical properties of soils used in this study are summarized in Table 1.

Table 1. Properties of sand and clay used in this study

	K3	K4	K5	Kaolinite	Illite	Bentonite
G_s	2.65	2.65	2.65	2.47	2.71	2.12
e_{max}	0.98	0.97	0.96	-	-	-
e_{min}	0.69	0.70	0.71	-	-	-
d_{50} (mm)	1.7	1.22	0.83	15.17×10^{-3}	12.69×10^{-3}	9.96×10^{-3}
C_u	1.64	1.51	1.79	2.69	2.15	3.77
Roundness	0.71	0.78	0.76	-	-	-
SR_{K3}	-	-	-	112.06	133.96	170.68
SR_{K4}	-	-	-	80.42	96.14	122.49
SR_{K5}	-	-	-	54.71	65.41	83.33

Note: G_s = specific gravity; e_{max} = maximum void ratio; e_{min} = minimum void ratio; d_{50} = median grain size; C_u = coefficient of uniformity defined as d_{60}/d_{10}, where d_{60} and d_{10} are the diameters corresponding to 60% and 10% finer in the PSDs; R=roundness, respectively.

2.2 *Two-dimensional flow cell*

To perform the suffusion experiments, an acrylic cell with a height, width, and length of 0.2, 0.03, and 0.32 m was designed (wall thickness = 0.015 m). The designed cell was divided into an inlet, a sample, and an outlet as shown in Figure 1. To minimize the pulsation effect caused by the peristaltic pump, the dampener was designed with a length of 0.12 m, which is filled with background solution during the experiment. The two thin acrylic plates with 448 holes (diameter = 2.3 mm) and 66 holes (diameter = 5 mm) were installed between the inlet and sample part for distributing the flow throughout the cross-sectional area of the sample. To prevent the loss of sand during the injection, plastic mesh with an opening size of 0.25 mm (corresponding to #60 sieve) was installed at the inlet and outlet. Three outlets were installed at distances of 5 mm, 85 mm, and 165 mm above the base to evaluate the suffusion of clay particles and the critical hydraulic gradient as a function of depth.

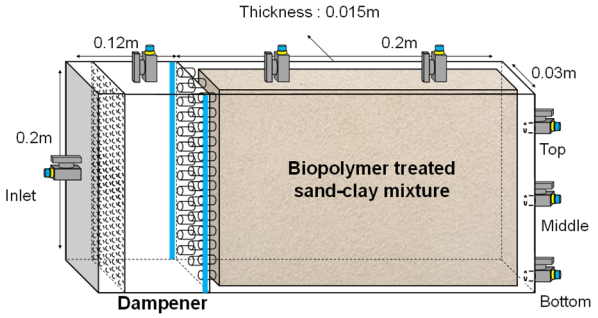

Figure 1. Two-dimensional flow cell

2.3 *Sample preparation and experimental setup*

The sand was mechanically washed multiple times until the turbidity of the suspension was reduced to below 10 NTU. The impurities attached to the sand were then removed using a sonicator bath (frequency = 40 kHz) by placing the container filled with sand and water. The oven-dried sand was mixed with 3% of clay by weight for 30 min to ensure a homogenous mixing state of the sand-illite mixture. A wet pluviation method was employed to prepare the saturated sand-clay mixtures. A dry sand-clay mixture with a relative density of 70%, based on pure sand, was introduced into the flow cell using a funnel. The end of the funnel was submerged in the biopolymer solution (background solution for untreated sand-clay mixtures). After completing the sample preparation, the remaining air at the top of the flow cell was entirely removed using the three saturation valves installed at the top of the flow cell (Figure 1).

The biopolymer concentrations for treating sand-illite mixtures were selected as 0.005%, 0.01%, 0.05%, and 0.1% by weight. The biopolymer was added to water and subsequently stirred using a hotplate magnetic stirrer with the temperature at the hotplate ~ 150°C until complete dissolution was achieved. Then, the biopolymer solution was placed in ambient conditions until it reached a room temperature of 20°C.

A programmable peristaltic pump was used to linearly increase the flow rate from 0.1 to 170 mL/min (corresponding to the Darcy's velocity of 0.0167 to 28.33 mm/min) at an increase rate of 0.1 mL/min per second. The heights of the three outlets were kept identical to eliminate the effects of head differences between the inlet and outlets during the injection process, ensuring that the initial flow rates at the three outlets were identical (e.g., 0.1 mL/min in each outlet for the flow rate of 0.3 mL/min).

An automatic turbidimeters were installed at the three outlets to measure the continuous turbidity of the filtrated clay during the injection and to determine the i_{cr}. Note that the hydraulic gradient at a turbidity of 60 NTU (i.e., ~ 80 mg/L of illite) was defined as i_{cr} in this study (Israr & Indraratna 2019).

From the observed breakthrough curves (BTC), the fraction of filtrated clay (M_e) using the trapezoidal method (calculating area under the observed BTC (Figure 2)) was evaluated for the quantitative representation of suffusion for all experimental conditions. In addition, the particle size distribution of the filtrated clay at the three outlets was evaluated using the particle size analyzer (Horiba LA-960).

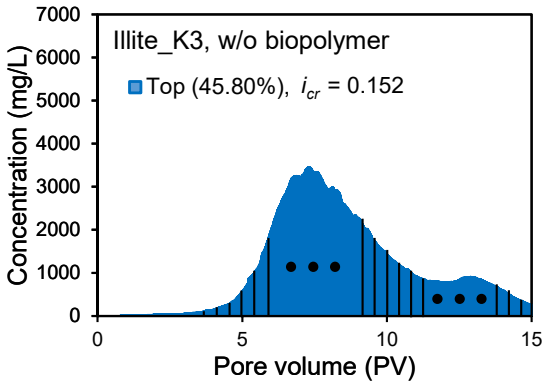

Figure 2. Calculation of M_e values using trapezoidal method

3 RESULTS AND DISCUSSION

3.1 *Critical hydraulic gradient and suffusion*

As seen in Figure 3, non-swelling clay (illite, kaolinite) exhibited higher M_e values than swelling clay (bentonite), with illite mixtures showing the highest M_e values across all IC conditions. It was found that the susceptibility to suffusion followed the order of illite, kaolinite, and bentonite in this study (Figure 3).

As the SR between sand and clay decreases (i.e. lower particle sizes of sand), stronger hydrodynamic forces are applied to the clay particles, which promote their detachment and transport through the pores, leading to higher M_e values. In addition, low IC (i.e. IC = 0 M) induces suffusion due to dominant repulsive electrostatic forces between sand and clay. As IC increases, the attractive forces between clay particles and sand grains become high, leading to increased chance of reattached illite particles and reduction of suffusion. Therefore, lower M_e values at IC = 0.01 M (Figure 4) than IC = 0 M was observed in this study.

A lower i_{cr} (i.e. earlier initiation of suffusion) does not necessarily correspond to a higher M_e value, indicating that early filtration of clay particles does not always lead to long-term suffusion. In addition, the order of flow rate (data not shown here) during the injection at the top, middle, and bottom outlets was reversely consistent with the order of i_{cr} at IC = 0 M, implying that the flow rate can be a useful indicator of assessing i_{cr} at the low IC. However, this may not be valied at high IC, likely because of increased reattachment effects. The observed BTCs in this study compared to those in the previous study (Won & Joo, 2024) imply that the gradual increase in flow rate leads to more significant suffusion than the constant flow rate at the given IC for sand-clay mixtures.

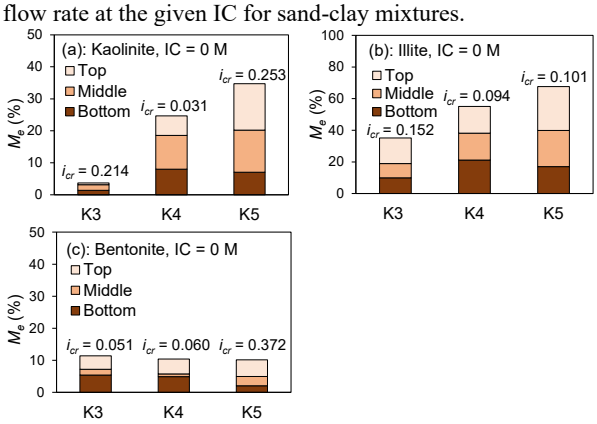

Figure 3. M_e values at top, middle, and bottom outlets for all experimental conditions under IC = 0 M. The i_{cr} value represents the minimum i_{cr} among the top, middle, and bottom outlets.

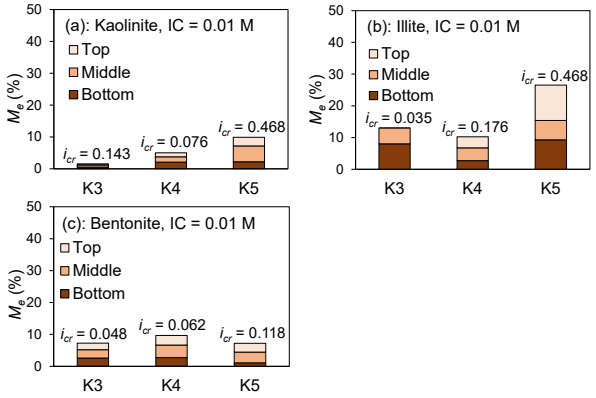

Figure 4. M_e values at top, middle, and bottom outlets for all experimental conditions under IC = 0.01 M. The i_{cr} value represents the minimum i_{cr} among the top, middle, and bottom outlets.

3.2 *Biopolymer-treated sand-clay mixtures*

As seen in Figure 5, among the tested biopolymers, guar gum exhibited the most substantial mitigation of suffusion, followed by chitosan, agar gum, xanthan gum, and gellan gum, in descending order (Figure 5). Notably, gellan gum treatment resulted in greater suffusion than the untreated sample, highlighting that biopolymer treatment does not always lead to the mitigation of suffusion.

Xanthan gum-treated samples exhibited early breakthrough of illite particles across all concentrations, with relatively low clay filtration at 0.005% and 0.01%. However, at higher concentrations (0.05% and 0.1%), increased viscosity led to preferential flow paths and high M_e values (Figure 5(a)), as flow-induced alignment of xanthan chains likely reduced structural entanglement. Therefore, xanthan gum concentrations exceeding 0.05% are not recommended for suffusion mitigation of sand-clay mixtures.

Agar gum showed optimal suffusion mitigation at agar gum concentration of 0.05% (Figure 5(b)), which can be attributed to its gelation behavior and viscoelastic stability in the 0.02-0.1% concentration range. At agar gum concentration = 0.1%, an increase in illite filtration was observed, likely due to excess agar molecules forming weak flocs in the aqueous phase. Hence, precise control of agar gum dosage is critical for achieving effective mitigation of suffusion.

Gellan gum was found to be ineffective for suffusion mitigation as inferred from high M_e values across all tested gellan gum concentrations (Figure 5(c)). Particularly gellan gum concentration = 0.1% shows the highest peak illite filtrate concentration (~5000 mg/L) among all cases. The M_e values at 0.01%, 0.05%, and 0.1% were higher than those of the untreated sample, indicating that more significant suffusion occurred by zellan gum treatment than in the untreated sample. This poor performance is attributed to the lack of ionic cross-linking in deionized water, which prevented gellan gum from forming stable gel structures.

Chitosan demonstrated excellent performance at 0.005-0.05%, which can be attributed to strong electrostatic interactions between its protonated amine groups and the negatively charged surfaces of illite particles. However, overdosing at 0.1% led to a sudden rise in M_e value (Figure 5(d)), likely due to charge reversal, which represents the formation of loosely bound flocs caused by a shift from cationic to anionic surface charge of chitosan.

Guar gum exhibited outstanding suffusion mitigation across all treated concentrations, with negligible filtrated illite concentration and M_e values lower than 1%. This performance is attributed to its strong bonding capacity and resilient polymer structure, which maintains stable interparticle cohesion even under increasing flow. In addition, its relatively low cost makes it a highly practical option for suffusion mitigation.

The i_{cr} generally decreased with biopolymer treatment (Figure 6), compared to the untreated sample. This trend was particularly evident in xanthan and agar gum-treated samples. However, lower i_{cr} does not necessarily correspond to greater suffusion, as indicated by low M_e values in guar gum and chitosan treatments.

The flow rate-dependent suffusion behavior strongly depends on biopolymer type. Xanthan gum and agar gum treatments showed higher M_e values at 0-5 PV (Figures 5(a) and 5(b)), indicating early-stage suffusion. In contrast, gellan gum, chitosan, and guar gum treatments exhibited high M_e values after 5 PV, suggesting that suffusion in these cases mainly occurred at high flow rates.

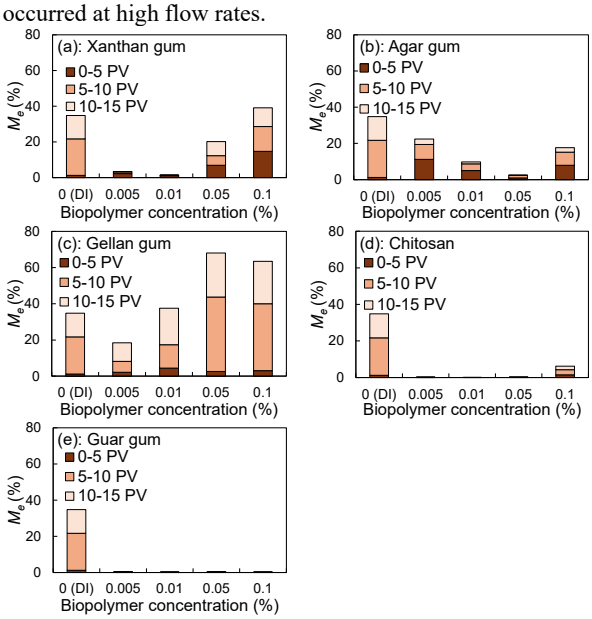

Figure 5. M_e values according to pore volume.

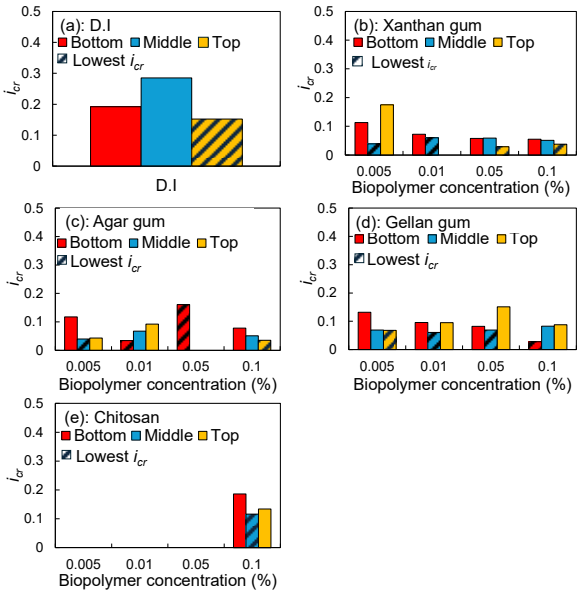

Figure 6. i_{cr} values by biopolymer treatment concentration. The hatched bars represent the lowest i_{cr} values.

4 CONCLUSIONS

This study investigated the suffusion behavior of sand-clay mixtures under a gradual increase in flow rate. In addition, the

mitigation of suffusion by biopolymer treatment was assessed. The key findings are summarized as follows.

1) Higher M_e values in sand-illite mixtures compared to sand-kaolinite and sand-bentonite mixtures under all IC conditions suggest that illite-containing soils are more susceptible to suffusion.
2) Swelling clay demonstrated low suffusion due to strong reattachment driven by its high swelling potential and the influence of gravity.
3) The comparison of i_{cr} and M_e values across the top, middle, and bottom outlets suggests that earlier initiation of suffusion does not lead to more significant suffusion.
4) The significant mitigation of suffusion by biopolymer treatment was observed in this study. Guar gum-treated sample showed the highest mitigation efficiency, followed by chitosan-, agar gum-, xanthan gum-, and gellan gum-treated samples.
5) Guar gum provided the most consistent and effective suffusion mitigation across all treated concentrations, with M_e values lower than 1%.

5 ACKNOWLEDGEMENTS

This research was supported by the National Research Foundation of Korea (NRF) Grants funded by the Korean government (No. RS-2022-NR071877 and RS-2026-25467870).

6 REFERENCES

Adamo, N., Al-Ansari, N., Sissakian, V., Laue, J., and Knutsson, S. (2020). Dam Safety: Technical Problems of Aging Embankment Dams: *Journal of Earth Sciences and Geotechnical Engineering*, Vol. 10, No. 6, pp. 1792–9660.

Chen, L., Wan, Y., He, J.J., Luo, C.M., Yan, S.F., and He, X.F. (2021). *Experimental study on the suffusion mechanism of gap-graded soils under an exceedance hydraulic gradient*, Springer Netherlands.

Fannin, R.J., and Slangen, P. (2014). On the distinct phenomena of suffusion and suffosion: *Proceedings of the Institution of Civil Engineers: Structures and Buildings*, Vol. 4, pp. 289–294, DOI: 10.1680/geolett.14.00051.

Hunter, R.P., and Bowman, E.T. (2018). Visualisation of seepage-induced suffusion and suffosion within internally erodible granular media: *Geotechnique*, Vol. 68, No. 10, pp. 918–930, DOI: 10.1680/jgeot.17.P.161.

Israr, J., and Indraratna, B. (2019). Study of Critical Hydraulic Gradients for Seepage-Induced Failures in Granular Soils: *Journal of Geotechnical and Geoenvironmental Engineering*, Vol. 145, No. 7, pp. 1–15, DOI: 10.1061/(asce)gt.1943-5606.0002062.

Ke, L., and Takahashi, A. (2014). Experimental investigations on suffusion characteristics and its mechanical consequences on saturated cohesionless soil: *Soils and Foundations*, Vol. 54, No. 4, pp. 713–730, DOI: 10.1016/j.sandf.2014.06.024.

Nam, B.H. (2019). Special Contribution Detection and Geotechnical Characterization of Sinkhole: Central Florida Case Study: Vol. 4, No. 3, pp. 9–14.

Parekh, M.L. (2016). *Advancing internal erosion monitoring using seismic methods in field and laboratory studies*, Colorado School of Mines.

Tao, H., and Tao, J. (2017). Numerical Modeling and Analysis of Suffusion Patterns for Granular Soils: No. March 2017, pp. 487–496, DOI: 10.1061/9780784480472.051.

Wan, C.F., and Fell, R. (2008). Assessing the Potential of Internal Instability and Suffusion in Embankment Dams and Their Foundations: *Journal of Geotechnical and Geoenvironmental Engineering*, Vol. 134, No. 3, pp. 401–407, DOI: 10.1061/(asce)1090-0241(2008)134:3(401).

Won, J., Choe, Y., Yang, Y., and Choi, H. (2023). Impact of clay particle reattachment on suffusion of sand-clay mixtures: *Journal of Rock Mechanics and Geotechnical Engineering*, Vol. 15, No. 10, pp. 2720–2730, DOI: 10.1016/j.jrmge.2022.12.013.

Won, J., and Joo, I. (2024). Two-dimensional experimental assessment of interaction energy-induced suffusion in sand-clay mixtures: *Geotechnique*, DOI: 10.1680/jgeot.23.00265.

Xiong, H., Wu, H., Bao, X., and Fei, J. (2021). Investigating effect of particle shape on suffusion by CFD-DEM modeling: *Construction and Building Materials*, Vol. 289, p. 123043, DOI: 10.1016/j.conbuildmat.2021.123043.

Xu, Z., Lin, P., Xing, H., and Wang, J. (2021). Mathematical modelling of cumulative erosion ratio for suffusion in soils: *Proceedings of the Institution of Civil Engineers: Geotechnical Engineering*, Vol. 174, No. 3, pp. 241–251, DOI: 10.1680/jgeen.19.00082.